

Original Study

Open Access

Abolghasem Ahmadi, Mohammad Amin Nozari, Meysam Bayat\*, Ehsan Delavari

# Investigating Calcareous and Silica Sand Behavior at Material Interfaces: A Comprehensive Study

<https://doi.org/10.2478/sgem-2024-0023>

received October 27, 2023; accepted August 25, 2024.

**Abstract:** This study centers on the crucial determination of the mobilized friction angle between soil and various materials, including steel and concrete, to enhance the modeling of soil-structure interaction. The primary objective of the current investigation was to assess the interfacial friction between calcareous and silica sands when interacting with concrete or steel surfaces. To achieve this, direct shear tests were conducted to examine the impacts of relative density ( $Dr$ ), surface roughness ( $Rn$ ), and shearing direction. The test results reveal that the shear strength of calcareous sand surpasses that of silica sand when considering a specific  $Rn$ . Furthermore, the interface friction of both sand types escalates with an increase in normal stress and  $Rn$ , with higher values observed in interactions with steel plates. Notably, the friction angle ratio (the interaction friction angle over the pure sand friction angle) demonstrates minimal dependence on the sand type. The most pronounced divergence in the friction angle ratio is evident at the maximum  $Rn$  value, which increases alongside  $Rn$  values for both calcareous and siliceous sands. With increasing  $Rn$  values, the maximum shear strength, contingent on normal stress and relative density, also rises. The influence of relative density on the interaction friction angle diminishes with escalating surface roughness.

**Keywords:** Calcareous sand; Silica sand; Interface; Steel; Concrete; Direct shear test.

## 1 Introduction

The interaction between soil and various materials plays a pivotal role in numerous civil engineering applications, including pile foundations and soil reinforcement (Janipour et al., 2022; Motallebiyan et al., 2020; Noroozi et al., 2022a, 2022b; Vieira et al., 2013; Yavari et al., 2016). To date, extensive research has been conducted through field and laboratory tests, as well as numerical simulations, to delve into the interface between soil and different materials like geosynthetics, concrete, and steel (Farhadi and Lashkari, 2017; Guo et al., 2020; H. lei Kou et al., 2021; Liu et al., 2014; Mortazavi Bak et al., 2021; Wang and Richwien, 2002). Previous investigations have indicated that the interaction at the soil-material interface under static or cyclic loading is predominantly influenced by geotechnical properties of the soil (e.g., soil density, moisture content, grading characteristics of soil, and angularity of particles) and material properties (e.g., material type and surface roughness) (Arulrajah et al., 2015; Janipour et al., 2022; Khan et al., 2014; Kishida and Uesugi, 1987; Vangla and Latha Gali, 2016; Xiao et al., 2019).

The direct interface shear test, known for its simplicity and directness, is commonly used to study soil-structure interface behavior. Potyondy, (1961) carried out a series of direct shear tests to explore the mobilized friction between soils and structural materials, such as wood, concrete, and steel. These tests have revealed that geotechnical properties of soils, such as water content, the properties of structural materials (including surface roughness), and the level of normal stress primarily affect the mobilized interface friction. Kishida and Uesugi (1987) and Hammoud and Boumekik (2006) have emphasized the significant influence of steel surface roughness on the mobilized shear strength between geological materials and structural materials. Additionally, Gireesha and Muthukkumaran (2011) have noted an increase in both internal and interface friction angles with rising relative density of soils. Vieira et al. (2013) have studied soil-reinforcement interaction mechanisms through direct and simple shear

\*Corresponding author: Meysam Bayat, Department of Civil Engineering, Najafabad Branch, Islamic Azad University, Najafabad, Iran, E-mail: bayat.m@pci.iaun.ac.ir

Abolghasem Ahmadi, Department of Civil Engineering, Najafabad Branch, Islamic Azad University, Najafabad, Iran

Mohammad Amin Nozari, Department of Civil Engineering, Rasht Branch, Islamic Azad University, Rasht, Iran

Mohammad Amin Nozari, Ehsan Delavari, Department of Civil Engineering, Najafabad Branch, Islamic Azad University, Najafabad, Iran

tests, identifying soil and reinforcement characteristics as the most influential parameters. Furthermore, Yavari et al. (2016) have suggested that temperature exerts a negligible effect on the shear strength parameters of the soil-concrete interface. Janipour et al. (2022) have specifically examined the interface friction between sand and concrete using direct shear tests, revealing that the mobilized interface friction is affected by the relative density of sand, surface roughness, normal stress levels, and the area of interaction between concrete and sand at the shear boundary. Samanta et al. (2018) conducted a thorough assessment of interface shear strength between sand and construction materials, considering factors like surface roughness, particle size, and relative density when sand interfaces with steel or concrete. Han et al. (2018) explored the impact of factors like interface roughness, particle characteristics, and sand gradation on the friction angle at the interface. Su et al. (2018) investigated the effect of relative roughness ( $R_n$ ) and mean particle size ( $D_{50}$ ) on shear behavior at the sand-steel interface, finding a critical  $R_n$  value beyond which peak shear stress and friction angle did not increase. As mentioned before,  $R_n$  is defined as the ratio of the maximum vertical peak-to-valley distance ( $R_{max}$ ) to  $D_{50}$ . Kou et al., (2021) studied the impact of surface roughness and mean particle size on the friction behavior at the calcareous sand-steel interface, showing that greater roughness led to higher peak shear strength, with calcareous sand having a higher friction angle than siliceous sand. Uesugi and Kishida's laboratory tests revealed that the mean grain size of sand within the examined range did not significantly affect behavior (Uesugi and Kishida, 1986). Liu et al. (2019) used a cyclic direct shear apparatus to investigate pile-sand interfaces, providing insights into cyclic weakening mechanisms, including stress attenuation, strength reduction, and particle crushing, while also exploring the influence of initial conditions, shear deformation, and pile roughness. Rui et al. (2021) studied the cyclic behavior of the interface shear between carbonate sand and steel, considering factors such as cyclic amplitude, particle size, surface roughness, and normal stress, finding that cyclic shear increased interface strength compared to monotonic shear.

Despite this extensive research, most studies on the soil-material interface have predominantly focused on silica sand. Calcareous sand, a distinctive type of soil shaped by various biological and chemical influences, has received comparatively less attention. Prior investigations have indicated that calcareous sand is more prone to crushing than silica sand (Choo et al., 2020; Lei et al., 2020; Li et al., 2021a; Shahidi et al., 2024; Tao et al., 2021; Wang et al., 2022). Ha Giang et al.

(2017) have reported that grading characteristics, such as  $D_{50}$  and Coefficient of Uniformity ( $C_u$ ), significantly impact the mobilized friction angle between calcareous sand and steel. Rezvani, (2020) conducted a series of monotonic compression triaxial tests on calcareous sand, concluding that an increase in the number of horizontal geotextile layers reduces particle breakage in the sand. Li et al. (2020) have explored the potential of microbially induced carbonate precipitation to enhance the interface resistance between calcareous sand and steel. Wang et al. (2019) have investigated the effect of surface roughness on the interface between calcareous and silica sand and steel, revealing that the mobilized friction angle between the steel surface and calcareous sand is approximately 5 to 6 degrees than that observed with silica sand. (H. lei Kou et al., 2021) conducted a series of direct shear tests to study the influence of surface roughness and mean particle size of sand on the calcareous sand-steel interface, concluding that the interface friction angle is primarily dictated by the roughness of the steel plate, with calcareous sand exhibiting a higher friction angle compared to silica sand. Furthermore, Xu et al. (2022) pointed out that the interface peak internal friction angle of geogrid-reinforced calcareous sand is significantly greater than that of unreinforced calcareous sand.

To the best of current knowledge, no comparative study has been conducted to assess differences in the mobilized friction angle between silica and carbonate sands in their interactions with various structural materials such as steel and concrete. The principal aim of this research is to investigate the impact of steel or concrete surface roughness, relative density, and shearing angle relative to the direction of grooves on the interface shear strength between sand and steel or concrete surfaces. Additionally, this study delves into the crushing rate of calcareous sand.

## 2 Description of the Experimental Work

### 2.1 Materials

As illustrated in Figure 1, two distinct types of sand, namely silica and calcareous sand, were utilized in the study, both adhering to a specified grading curve. The investigation aimed to evaluate the interface shear strength between these sands and steel or concrete surfaces. Table 1 provides an overview of the physical and geotechnical properties of the sand materials employed. Both silica and calcareous sand fall under the classification of poorly

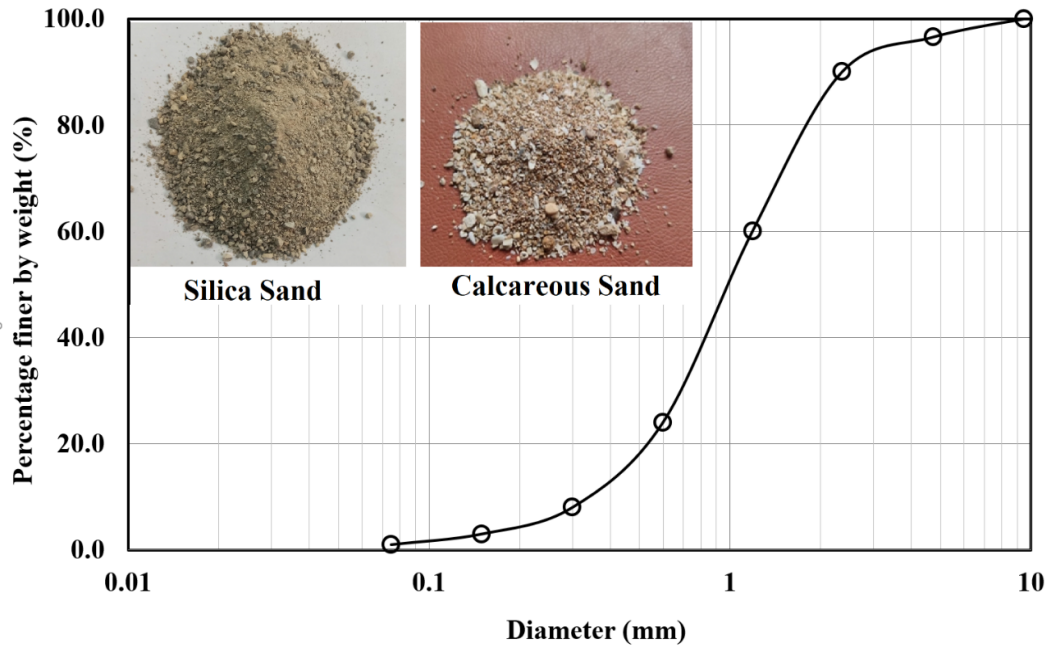


**Figure 1:** Grain size distribution curves and photographs of calcareous and silica sands.

**Table 1:** Physical and geotechnical properties of calcareous and silica sands.

Characteristics	Symbol	Unit	Calcareous Sand	Silica Sand
Specific Gravity	$G_s$	(-)	2.73	2.71
Particle Diameter at 10% Finer	$D_{10}$	(mm)	0.4	0.4
Particle Diameter at 30% Finer	$D_{30}$	(mm)	0.7	0.7
Particle Diameter at 50% Finer (mean particle size)	$D_{50}$	(mm)	1	1
Particle Diameter at 60% Finer	$D_{60}$	(mm)	1.19	1.19
Coefficient of Uniformity	$C_u$	(-)	2.98	2.98
Coefficient of Curvature	$C_c$	(-)	1.03	1.03
Minimum Void Ratio	$e_{min}$	(-)	0.61	0.54
Maximum Void Ratio	$e_{max}$	(-)	0.96	0.91
Maximum Dry Density	MDD	(g/cm <sup>3</sup> )	1.521	1.9
Optimum Moisture Content	OMC	(%)	4	8
Soil Type (Unified Soil Classification System)	UCSC	-	SP	SP

graded sand (SP). Notably, the visual examination of these sands reveals that calcareous sand exhibits a more angular particle morphology compared to silica sand. Table 2 presents the chemical properties of calcareous sand, which was sourced from Kish Island, situated in the Persian Gulf in southern Iran. X-ray fluorescence (XRF) analyses confirmed that Calcite is the principal component of Kish sand.

For the experimental setup, concrete and steel plates with varying degrees of  $R_n$  were utilized. Figure 2 provides a visual representation of steel plates with different  $R_n$  values.  $R_n$  denotes the ratio between the groove depth of the steel or concrete plate and the  $D_{50}$ . The concrete plates, as seen in the bottom row of Figure 2, were prepared using a mixture consisting of fine silica sand, ordinary Portland cement, and water, in a ratio of 1.8:3:1. These

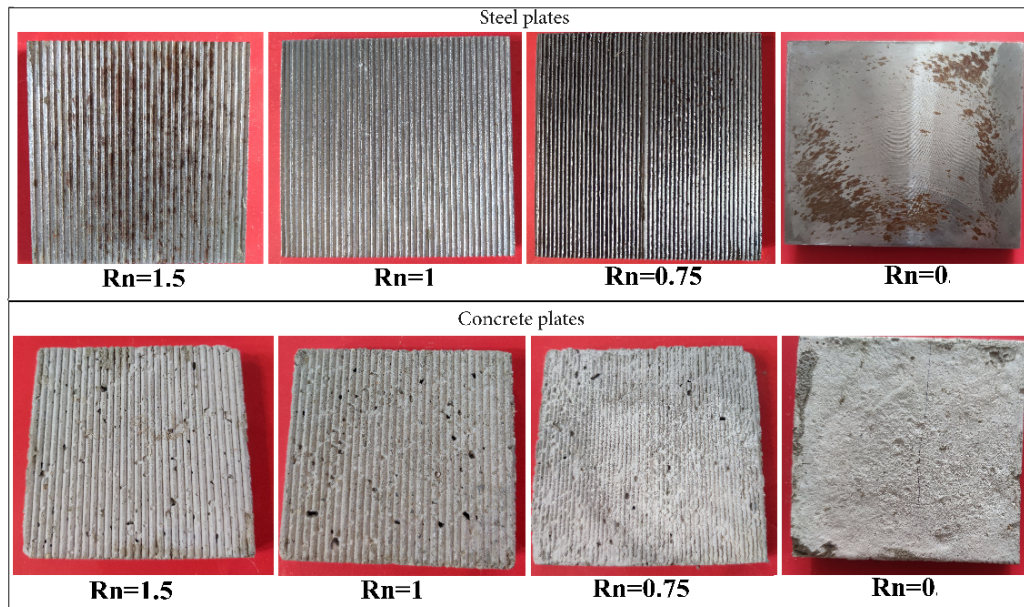


**Figure 2:** Steel and concrete plates with various  $Rn$  values.

**Table 2:** Chemical properties of calcareous sand.

Compound	Mass percentage (%)
CaO	50.03
MgO	1.630
SiO <sub>2</sub>	0.908
Na <sub>2</sub> O	0.796
SrO	0.580
Cl	0.525
SO <sub>3</sub>	0.500
Al <sub>2</sub> O <sub>3</sub>	0.270
Fe <sub>2</sub> O <sub>3</sub>	0.126
P <sub>2</sub> O <sub>5</sub>	0.091
K <sub>2</sub> O	0.066
CuO	0.021
LOI*	44.46

\* Loss on Ignition (1000 °C, 2 h)

concrete plates underwent a curing period of 28 days prior to the interface shear tests. The surfaces of both the steel and concrete plates were intentionally grooved prior to the direct shear tests. Each trench on the plates assumed an isosceles triangular cross-section, featuring varying heights in correspondence to the assigned  $Rn$  values and an apex angle of 45 degrees. It's worth noting that the

concrete plates exhibited localized damage following the direct shear tests and were used in just one test each. On the other hand, the steel plates remained undamaged throughout the testing. To achieve an  $Rn$  value of 0 for the concrete surface, a sanding process post-casting was implemented. This involved carefully sanding the surface of the concrete to significantly reduce its porosity and smooth out any roughness. The result was an almost smooth surface, comparable to that of steel, which allowed the  $Rn = 0$  condition to be met for the experiments.

## 2.2 Sample preparation and experimental procedure

The experimental approach encompassed a series of 10 × 10 cm direct shear tests conducted on prepared samples. To assemble the sand samples, dry sand was compacted within a box using tamping techniques to achieve the desired relative density. The tamping method employed a manual hammering device with a base area matching the sample surface (10 × 10 cm). This device featured a 1-kilogram weight attached to the base via a rod. The weight was lifted to a height of approximately 30 cm and then released, allowing it to hit the metal surface above the sample due to gravity. The entire amount of dry sand was poured into the mold and then compacted in one layer, considering the low thickness of approximately 3 centimeters in the upper part of the mold. The uniformity of the compacted sample was

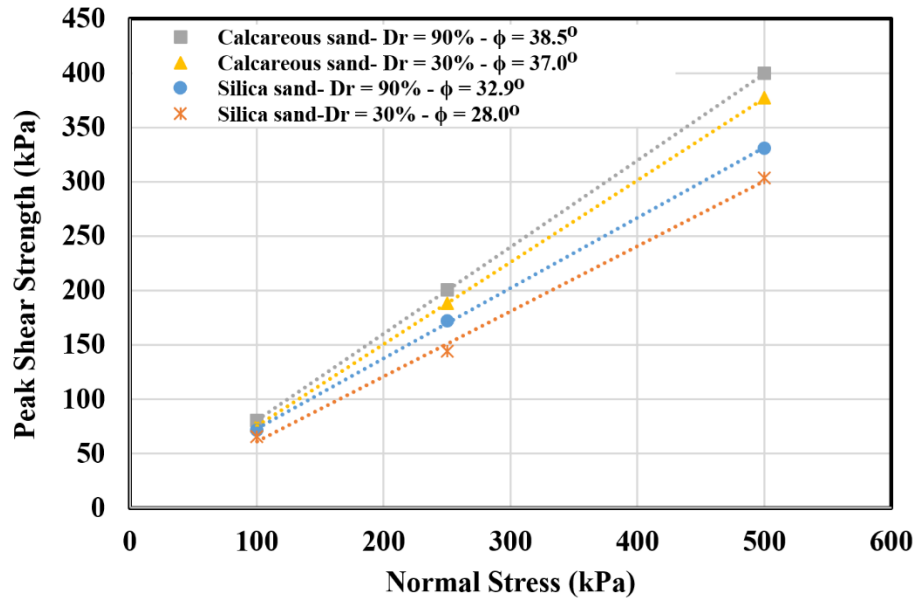


Figure 3: Shear strength envelopes for the tested soils at  $Dr$  of 30 and 90%.

ensured by maintaining consistent tamping procedures, resulting in an almost uniform density. The relative density was recalculated after applying the normal stress, and if the density change exceeded 5% relative to the desired relative density, the test was rejected, and the sample was remade to ensure accuracy.

For the interface tests, concrete or steel plates were positioned at the bottom section of the box, while the sand was compacted into the top section. It was essential to ensure precise alignment of the border between the plate and the sand on the shearing line. Following sample preparation, the specimens were subjected to a constant horizontal displacement rate of 1 mm/min in accordance with ASTM-D3080. To ascertain the shear strength parameters of the samples, direct shear tests were carried out under three different normal stress values: 100 kPa, 250 kPa, and 500 kPa.

Grain crushing can significantly impact calcareous sand, even at relatively low stress levels, potentially altering soil granulometry after shearing tests (Datta et al., 1979; Hakimelahi et al., 2023; Li et al., 2021b; Tavakol et al., 2023). While intending to assess grain crushing in the early stages of the experiments, the small size of the mold and the limited volume of sand used made accurate measurement challenging. To maintain consistency and reliability in the results, the sand was replaced with fresh, uncrushed samples after each shear test. This approach ensured that each test started with sand of consistent granulometry, mitigating the effects of particle crushing on the findings.

## 3 Results and Discussion

### 3.1 Interface behavior of calcareous and silica sand with steel

In the current study, calcareous and silica sands were employed at two distinct relative densities, 30% and 90%, to explore their interface characteristics with steel surfaces. Figure 3 illustrates the shear strength envelopes for both calcareous and silica sands, along with the corresponding friction angles. The findings reveal that calcareous sand exhibits friction angles approximately 17% and 32% higher than those observed with silica sand at relative densities of 30% and 90%. This disparity can be attributed to the inherent differences in particle morphology and surface texture between the two sands, with calcareous sand particles displaying a more angular and rougher surface, resulting in an elevated friction angle.

Within this section, the focus is on delving deeper into the mobilized friction angle between calcareous and silica sands and steel plates, particularly emphasizing tests conducted with calcareous and silica sand at a relative density of 90% and various  $R_n$ . Figure 4 presents the interaction shear strength envelopes for both sand types, showcasing the influence of changing  $R_n$  on the steel plates. It's notable that the variations in slope due to  $R_n$  changes in both sand types exhibit a similar trend. However, for equivalent  $R_n$  values, the shear strength

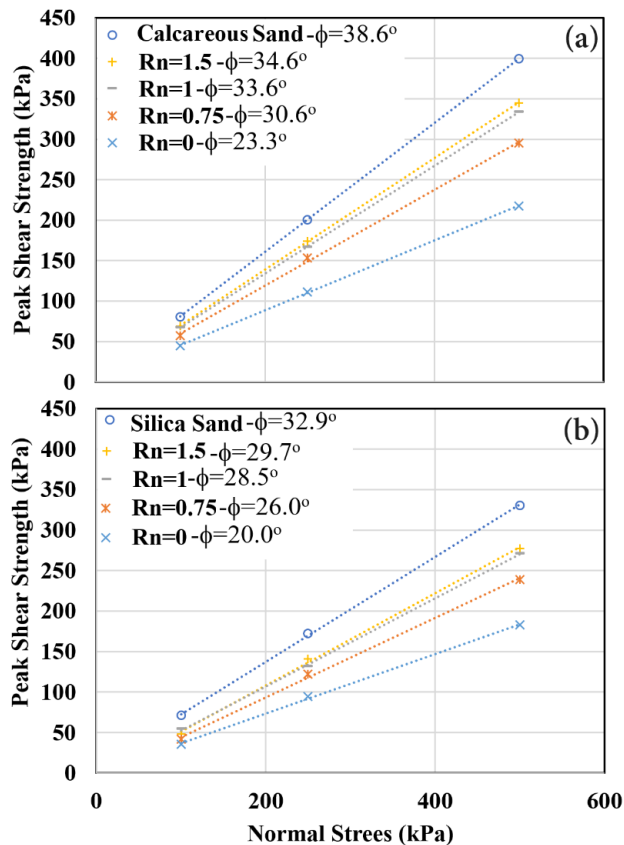


**Figure 4:** Shear strength envelopes for the interaction between (a) calcareous sand and steel plates, and (b) silica sand and steel plates, with different  $R_n$  values ( $Dr = 90\%$ ).

envelope for calcareous sand is slightly higher than that for silica sand. In Figure 4, the symbol  $\phi$  represents the mobilized friction angle at the interface between the soil (calcareous or silica sand) and the steel plates under the specified conditions when used after  $R_n$ . However, it indicates the internal friction angle when used after silica or calcareous sand.

Moving on to the maximum shear strength values, Figure 5 provides insights into the differences between calcareous and silica sands at various  $R_n$  values of the steel surface. The results highlight that calcareous sand consistently demonstrates higher shear strength compared to silica sand for a given  $R_n$  value. Moreover, this difference between the two sand types becomes more pronounced with increasing normal stress and  $R_n$  values.

The changes in the friction angle ratio were also scrutinized, representing the ratio of the mobilized friction angle at the sand-steel interface to the friction angle of the sand. Figure 6 demonstrates that this ratio remains relatively consistent, regardless of the sand type. Figure 6 provides insight into the variation of the friction

angle ratio ( $\phi_i/\phi_s$ ) which represents the ratio of mobilized friction angle at the calcareous sand-steel interface ( $\phi_i$ ) to friction angle of calcareous sand ( $\phi_s$ ). However, it does exhibit an increase with rising  $R_n$  values for both calcareous and silica sands, indicating the influence of surface roughness on the interface behavior.

### 3.2 Effect of relative density

To comprehensively examine the impact of relative density on the behavior of the calcareous sand-steel interface, the tests were conducted at two distinct relative densities, 30% and 90%, while varying the roughness of the steel surfaces ( $R_n$  values of 0, 0.75, 1, and 1.5). The outcomes, as depicted in Figure 7, showcase a noticeable increase in the slope of the shear strength envelopes as  $R_n$  values rise in both sets of tests. This trend underscores the heightened influence of  $R_n$  in cases of lower relative density, with the lines representing lower relative density exhibiting greater separation.

For a more detailed analysis of the interplay between relative density and  $R_n$ , the maximum shear strength values of the sand-steel interface are presented against  $R_n$  in Figure 8. Here, it becomes evident that the effect of  $R_n$  becomes more pronounced with increasing normal stress. Specifically, the lines representing a normal stress of 500 kPa exhibit steeper slopes compared to those corresponding to normal stresses of 100 and 250 kPa. Moreover, the discrepancy between the results of samples with relative densities of 30% and 90% widens as the normal stress value escalates from 100 to 500 kPa. This suggests that an increase in  $R_n$  leads to an enhanced maximum shear strength, a value intrinsically linked to normal stress and relative density.

Figure 9 provides insight into the variation of the friction angle ratio ( $\phi_i/\phi_s$ ) which represents the ratio of mobilized friction angle at the calcareous sand-steel interface ( $\phi_i$ ) to friction angle of calcareous sand ( $\phi_s$ ). Notably, all the recorded values are less than one, indicating that the friction angle at the calcareous sand-steel interface consistently remains smaller than that of calcareous sand. It is important to highlight that, for a given  $R_n$  value, the friction angle ratio is notably higher when the relative density is 90% compared to 30%. This underscores the significant impact of relative density, especially when  $R_n$  values are at the lower end of the spectrum. Recent studies, such as Feng et al. (2024), have explored the mobilized shear strength at the interface of silica sand and steel surfaces. Their findings indicated that with increasing  $R_n$ , in some cases, the mobilized friction

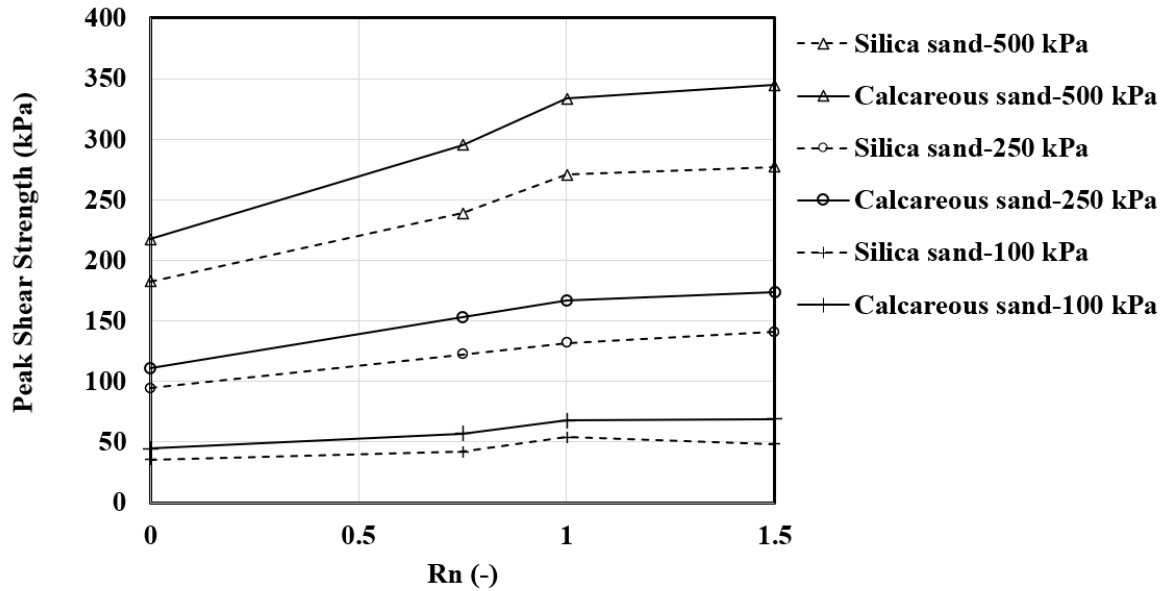


**Figure 5:** Maximum interface shear strength values between calcareous or silica sand and steel plates with various  $Rn$  values, under various normal stress levels and  $Dr = 90\%$ .

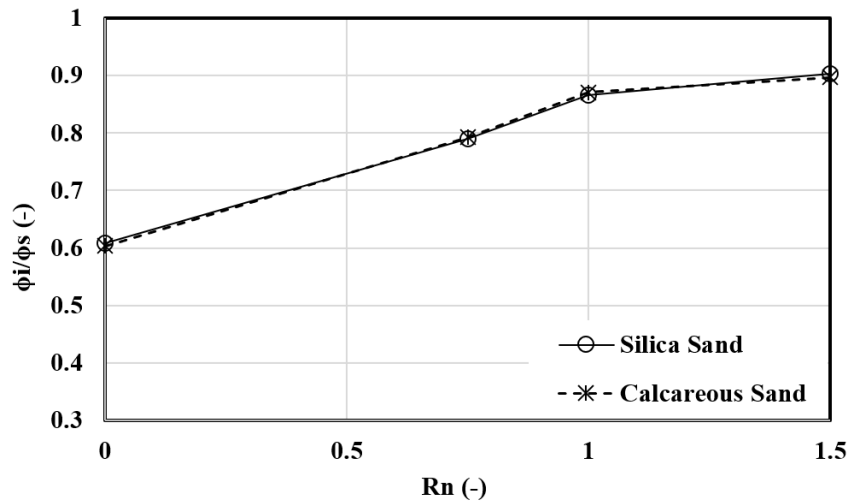


**Figure 6:** Friction angle ratios for both calcareous and siliceous sand ( $Dr = 90\%$ ).

angle at the sand-steel interface is higher than that of pure sand. This suggests that the ratio might indeed approach 1 or exceed it.

### 3.3 Behavior of calcareous sand at interfaces with steel and concrete

In an effort to discern the variations in how carbonate sand interacts with steel and concrete surfaces, the tests were done on the calcareous sand-concrete interface

at a consistent relative density of 90%. The  $Rn$  for the concrete plates matched that of the steel plates. The shear strength envelopes for the calcareous sand-concrete interface are depicted in Figure 10. Much like the findings in the calcareous sand-steel plate interface, an increase in  $Rn$  and normal stress elevates the maximum mobilized shear strength. In this case as well, heightened  $Rn$  values contribute to steeper slopes in the shear strength lines, mirroring the behavior observed in the calcareous sand-steel plate interface.

To further dissect the influence of steel and concrete plates, the maximum shear strength values for both plate types under various normal stress conditions are presented in Figure 11. These results unveil a nuanced relationship: for a constant normal stress and  $Rn$  values

exceeding 0.75, the mobilized shear strength at the sand-steel plate interface surpasses that of the sand-concrete plate interface. When  $Rn$  values are set at 0 and 0.75, the disparities between the results are negligible, and the outcomes remain largely independent of the plate material. However, as normal stress escalates, the distinctions between results obtained with  $Rn$  values of 1 and 1.5 become more pronounced, signifying the intricate interplay between surface roughness and plate material.

The variation of the friction angle ratio for the calcareous sand-concrete or steel interface at a relative density of 90% is illustrated in Figure 12. At an  $Rn$  value of zero, the friction angle ratio is marginally higher in the case of the concrete plate when compared to the steel plate. This divergence can be attributed to the unevenness of the concrete surface in contrast to the steel surface when  $Rn$  equals zero. However, for  $Rn$  values exceeding zero, the friction angle ratio for the steel plate exceeds that of the concrete plate. This shift can be ascribed to the sharper edges found on the steel surface in comparison to the concrete surface. The most significant discrepancy in the friction angle ratio is evident at the maximum  $Rn$  value, highlighting the importance of surface roughness in governing interface behavior.

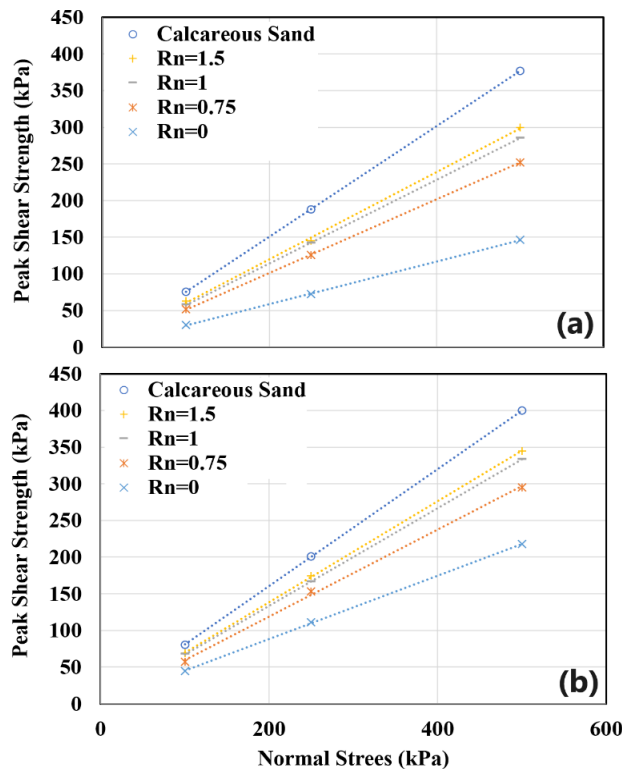


**Figure 7:** Shear strength envelopes for the calcareous sand-steel interface under (a)  $Dr = 30\%$  and (b)  $Dr = 90\%$  with various  $Rn$  values.

### 3.4 Influence of shearing direction

In this section, the effects of shearing direction on the interaction between calcareous sand and steel or concrete surfaces were examined through two sets of direct shear tests. Unlike previous tests where the angle between the shearing direction and grooves ( $\beta$ ) was fixed at 90

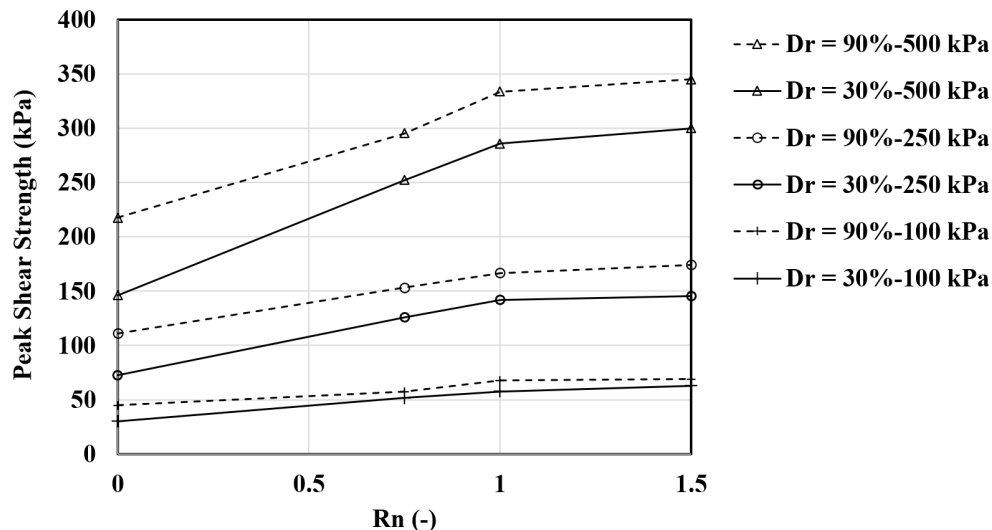


**Figure 8:** Maximum shear strength of the calcareous sand-steel interface versus the  $Rn$  under various normal stress levels.

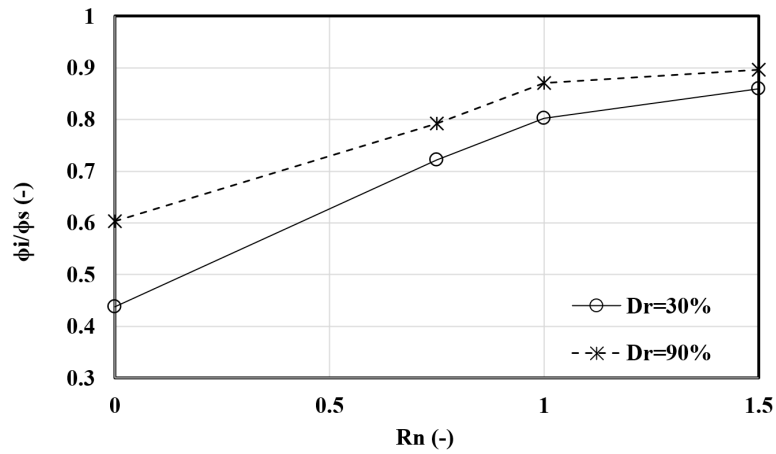


Figure 9: Variation of the friction angle ratio of calcareous sand-steel interface versus the  $R_n$  under  $D_r$  of 30 and 90%.

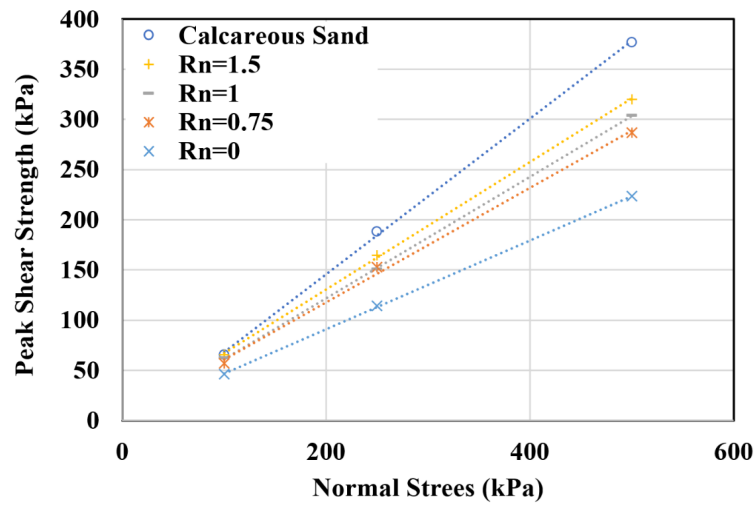


Figure 10: Shear strength envelopes of the calcareous sand-concrete interface.

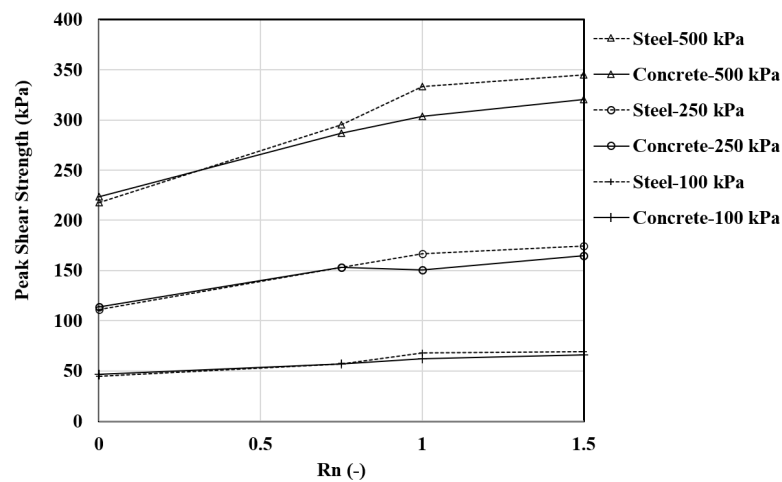
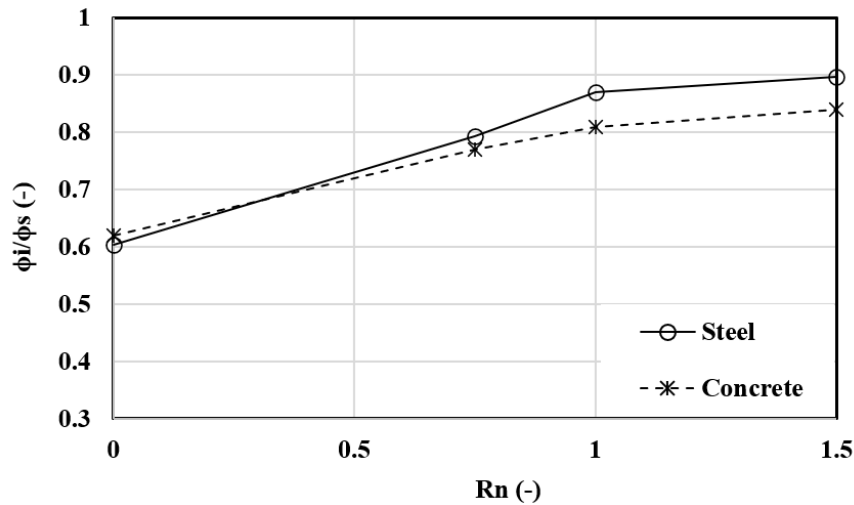
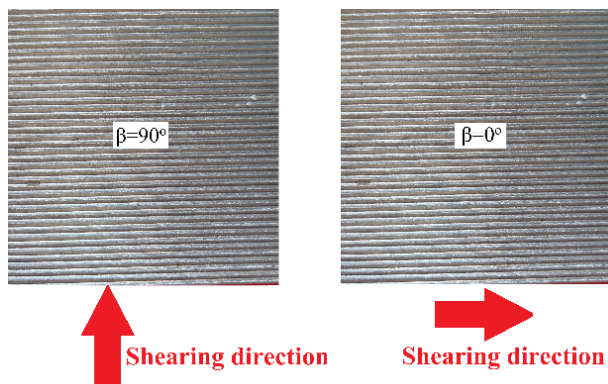


Figure 11: Maximum mobilized shear strength values at the interface of calcareous sand and steel or concrete plates under various normal stress values ( $D_r = 90\%$ ).



**Figure 12:** Friction angle ratio for calcareous sand-concrete or steel interface at  $Dr$  of 90%.



**Figure 13:** Shearing angles of 0° and 90°.

degrees,  $\beta$  was adjusted to zero degrees, as depicted in Figure 13, for these particular tests. The tests with plates in the perpendicular direction were conducted using sand with a  $Dr$  of 90%.

The results, presented in Figure 14, illustrate the impact of altering the shearing angle from 0 degrees to 90 degrees on the shear strength envelopes at the interface between calcareous sand and concrete and steel plates. In Figure 14, the symbol  $\phi$  represents the mobilized friction angle at the interface between the calcareous sand and the steel or concrete plates when written after steel or concrete. It represents the internal friction angle of calcareous sand when written after calcareous sand. Notably, an increase in the shearing angle leads to a steeper slope in the shear strength envelope. In all cases, the interaction shear strength envelopes fall below the shear strength envelope observed for pure sand. Furthermore, the discrepancy between the results at shearing angles of 0 degrees and

90 degrees becomes more pronounced as the normal stress increases. Additionally, it's worth noting that the influence of the shearing angle on the interaction shear strength envelopes is more pronounced for steel plates than for concrete plates. This observation underscores the significance of shearing direction in governing the interface behavior, with implications for different materials.

## 4 Conclusions

In summary, the in-depth exploration of the interface between calcareous sand and both steel and concrete surfaces have unveiled critical insights. The investigations encompassed variations in relative density ( $Dr$ ), surface roughness ( $Rn$ ), shearing direction, and the nature of the material involved, providing a holistic understanding of this intricate interaction.

1. **Effect of Relative Density:** The significance of relative density emerged as a central theme in the current study. Calcareous sand consistently demonstrated superior performance compared to silica sand, displaying notably higher friction angles across a wide spectrum of relative densities. Notably, the influence of  $Rn$  became increasingly pronounced with higher relative densities. The results emphasized that the discrepancy between the behavior of sands at relative densities of 30% and 90% became more pronounced as normal stress escalated.
2. **Influence of Material Type:** A pivotal aspect of the investigation involved the comparison between the

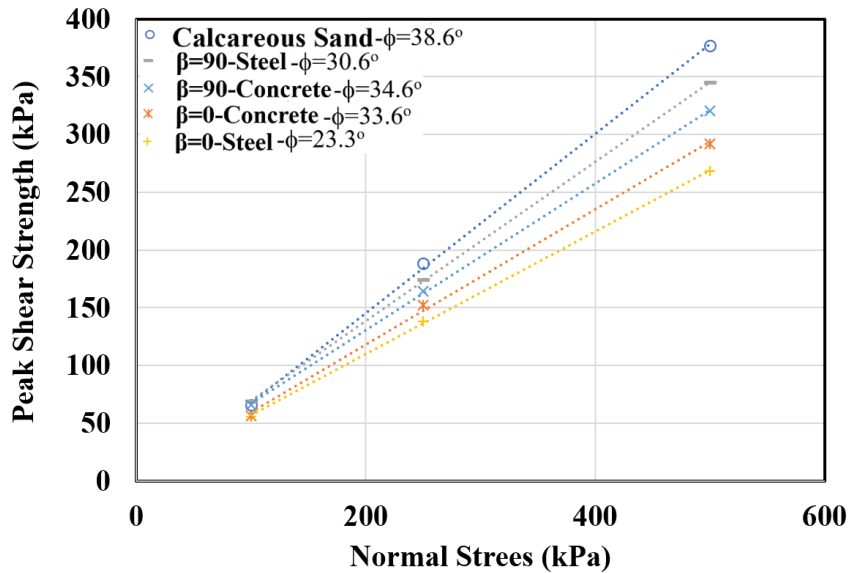


**Figure. 14:** Effect of shearing angle on the shear strength envelopes at the interface of calcareous sand and concrete or steel plates ( $Dr = 90\%$ ).

calcareous sand-steel and calcareous sand-concrete interfaces. It was found that when  $Rn$  values exceeded 0.75, the mobilized shear strength at the sand-steel interface consistently outperformed that of the sand-concrete interface. This disparity became more pronounced with increasing normal stress. These findings underscore the nuanced interplay between material types and surface roughness in governing interface behavior.

3. **Shearing Direction:** The intriguing influence of shearing direction was explored by varying the shearing angle from 0 degrees to 90 degrees. The results revealed that increasing the shearing angle resulted in steeper shear strength envelopes. Importantly, in all cases, the interaction shear strength envelopes consistently remained below the shear strength envelope observed for pure sand. This effect was more pronounced for steel plates compared to concrete plates, highlighting the intricate nature of shearing direction's impact on interface behavior.

In sum, this comprehensive study enhances the understanding of the complex factors that govern the behavior of calcareous sand at material interfaces. The practical implications of these findings extend to a multitude of civil engineering applications, particularly in projects that involve pile foundations and soil reinforcement, where precise comprehension of soil-material interaction is paramount. Future research endeavors could delve further into additional factors and

materials, broadening the scope of knowledge and further refining models for soil-structure interaction.

## Data Availability

No data, models, or code were generated or used during the study

## References

- [1]. Arulrajah, A., Horpibulsuk, S., Maghoolpilehrood, F., Samingthong, W., Du, Y.J., Shen, S.L., 2015. Evaluation of interface shear strength properties of geogrid reinforced foamed recycled glass using a large-scale direct shear testing apparatus. *Advances in Materials Science and Engineering* 2015, 38–41. <https://doi.org/10.1155/2015/235424>
- [2]. Choo, H., Kwon, M., Touiti, L., Jung, Y.H., 2020. Creep of calcareous sand in Tunisia: effect of particle breakage at low stress level. *International Journal of Geo-Engineering* 11. <https://doi.org/10.1186/s40703-020-00123-2>
- [3]. Datta, M., Gulhati, S.K., Rao, G.V., 1979. Crushing of calcareous sands during shear, in: *Offshore Technology Conference*. OTC, p. OTC-3525.
- [4]. Farhadi, B., Lashkari, A., 2017. Influence of soil inherent anisotropy on behavior of crushed sand-steel interfaces. *Soils and Foundations* 57, 111–125. <https://doi.org/10.1016/j.sandf.2017.01.008>
- [5]. Feng, W.-Q., Bayat, M., Mousavi, Z., Li, A.-G., Lin, J.-F., 2024. Shear strength enhancement at the sand-steel interface: A pioneering approach with Polyurethane Foam Adhesive (PFA). *Construction and Building Materials* 429, 136297.

- [6]. Gireesha, N., Muthukumar, K., 2011. Study on soil structure interface strength property [WWW Document]. *Int J Earth Sci Eng*. URL <http://www.kluniversity.in/ace-klu/img/020410123.pdf> (accessed 3.6.21).
- [7]. Guo, J., Wang, X., Lei, S., Wang, R., Kou, H., Wei, D., 2020. Effects of Groove Feature on Shear Behavior of Steel-Sand Interface. *Advances in Civil Engineering* 2020. <https://doi.org/10.1155/2020/9593187>
- [8]. Ha Giang, P.H., Haegeman, W., Van Impe, P., Van Impe, W., Menege, P., 2017. Shear and interface shear strengths of calcareous sand. *ICSMGE 2017 - 19th International Conference on Soil Mechanics and Geotechnical Engineering* 377–380.
- [9]. Hakimelahi, N., Bayat, M., Ajalloeian, R., Nadi, B., 2023. Effect of woven geotextile reinforcement on mechanical behavior of calcareous sands. *Case Studies in Construction Materials* 18, e02014. <https://doi.org/10.1016/j.cscm.2023.e02014>
- [10]. Hammoud, F., Boumekik, A., 2006. Experimental Study of the Behaviour of Interfacial Shearing Between Cohesive Soils and Solid Materials At Large Displacement, *Asian Journal of Civil Engineering (Building and Housing)*.
- [11]. Han, F., Ganju, E., Salgado, R., Prezzi, M., 2018. Effects of Interface Roughness, Particle Geometry, and Gradation on the Sand–Steel Interface Friction Angle. *J. Geotech. Geoenviron. Eng.* 144, 04018096. [https://doi.org/10.1061/\(ASCE\)GT.1943-5606.0001990](https://doi.org/10.1061/(ASCE)GT.1943-5606.0001990)
- [12]. Janipour, A.K., Mousivand, M., Bayat, M., 2022. Study of interface shear strength between sand and concrete. *Arabian Journal of Geosciences* 15, 1–9. <https://doi.org/10.1007/s12517-021-09394-0>
- [13]. Khan, E.K., Ahmad, I., Ullah, A., Ahmad, W., Ahmad, B., 2014. Small and large scale direct shear tests on sand-concrete Interface. *The 1st International Conference on Emerging Trends in Engineering, Management and Sciences* 2014.
- [14]. Kishida, H., Uesugi, M., 1987. Tests of the interface between sand and steel in the simple shear apparatus. *Geotechnique* 37, 45–52. <https://doi.org/10.1680/geot.1987.37.1.45>
- [15]. Kou, H., lei, Diao, W., Zhou, Zhang, W., chun, Zheng, J., bin, Ni, P., JANG, B.A., Wu, C., 2021. Experimental Study of Interface Shearing between Calcareous Sand and Steel Plate Considering Surface Roughness and Particle Size. *Applied Ocean Research* 107, 102490. <https://doi.org/10.1016/j.apor.2020.102490>
- [16]. Kou, H., Diao, W., Zhang, W., Zheng, J., Ni, P., Jang, B.-A., Wu, C., 2021. Experimental Study of Interface Shearing between Calcareous Sand and Steel Plate Considering Surface Roughness and Particle Size. *Applied Ocean Research* 107, 102490. <https://doi.org/10.1016/j.apor.2020.102490>
- [17]. Lei, X., Lin, S., Meng, Q., Liao, X., Xu, J., 2020. Influence of different fiber types on properties of biocemented calcareous sand. *Arabian Journal of Geosciences* 13, 1–9. <https://doi.org/10.1007/s12517-020-05309-7>
- [18]. Li, Y., Li, B., Gong, J., 2021a. Revisiting the liquefaction resistance of calcareous sand using X-ray CT. *Soil Dynamics and Earthquake Engineering* 140, 106428. <https://doi.org/10.1016/j.soildyn.2020.106428>
- [19]. Li, Y., Lin, Z., Li, B., He, L., Gong, J., 2021b. Effects of gradation and grain crushing on the liquefaction resistance of calcareous sand. *Geomech. Geophys. Geo-energ. Geo-resour.* 7, 12. <https://doi.org/10.1007/s40948-020-00208-3>
- [20]. Li, Yujie, Guo, Z., Wang, L., Li, Yilong, Liu, Z., 2020. Shear resistance of MICP cementing material at the interface between calcareous sand and steel [WWW Document]. *Materials Letters*. <https://doi.org/10.1016/j.matlet.2020.128009>
- [21]. Liu, J.W., Cui, L., Zhu, N., Han, B., Liu, J., 2019. Investigation of cyclic pile-sand interface weakening mechanism based on large-scale CNS cyclic direct shear tests. *Ocean Engineering* 194, 106650. <https://doi.org/10.1016/j.oceaneng.2019.106650>
- [22]. Liu, Jiankun, Lv, P., Cui, Y., Liu, Jingyu, 2014. Experimental study on direct shear behavior of frozen soil-concrete interface. *Cold Regions Science and Technology* 104–105, 1–6. <https://doi.org/10.1016/j.coldregions.2014.04.007>
- [23]. Mortazavi Bak, H., Kariminia, T., Shahbodagh, B., Rowshanzamir, M.A., Khoshghalb, A., 2021. Application of biocementation to enhance shear strength parameters of soil-steel interface. *Construction and Building Materials* 294, 123470. <https://doi.org/10.1016/j.conbuildmat.2021.123470>
- [24]. Motallebiyan, A., Bayat, M., Nadi, B., 2020. Analyzing the Effects of Soil-Structure Interactions on the Static Response of Onshore Wind Turbine Foundations Using Finite Element Method. *Civil Engineering Infrastructures Journal* 53, 189–205. <https://doi.org/10.22059/ceij.2020.281914.1586>
- [25]. Noroozi, A.G., Ajalloeian, R., Bayat, M., 2022a. Experimental study of the role of interface element in earth dams with asphalt concrete core - Case study: Mijran dam. *Case Studies in Construction Materials* 16, e01004. <https://doi.org/10.1016/j.cscm.2022.e01004>
- [26]. Noroozi, A.G., Ajalloeian, R., Bayat, M., 2022b. Effect of FTC on the interface between soil materials and asphalt concrete using a direct shear test. *Case Studies in Construction Materials* 17, e01632. <https://doi.org/10.1016/j.cscm.2022.e01632>
- [27]. Potyondy, J.G., 1961. Skin friction between various soils and construction materials. *Geotechnique* 11, 339–353. <https://doi.org/10.1680/geot.1961.11.4.339>
- [28]. Rezvani, R., 2020. Shearing response of geotextile-reinforced calcareous soils using monotonic triaxial tests. *Marine Georesources and Geotechnology* 38, 238–249. <https://doi.org/10.1080/1064119X.2019.1566936>
- [29]. Rui, S., Wang, L., Guo, Z., Zhou, W., Li, Y., 2021. Cyclic behavior of interface shear between carbonate sand and steel. *Acta Geotech.* 16, 189–209. <https://doi.org/10.1007/s11440-020-01002-x>
- [30]. Samanta, M., Punetha, P., Sharma, M., 2018. Influence of surface texture on sand–steel interface strength response. *Géotechnique Letters* 8, 40–48. <https://doi.org/10.1680/jgele.17.00135>
- [31]. Shahidi, S., Bayat, M., Zareei, S.A., 2024. Enhancing Mechanical Behavior of Silica and Calcareous Sand through Polyurethane Foam, Nanomaterial, and Fiber. *Indian Geotech J.* <https://doi.org/10.1007/s40098-024-00971-0>
- [32]. Su, L.-J., Zhou, W.-H., Chen, W.-B., Jie, X., 2018. Effects of relative roughness and mean particle size on the shear strength of sand-steel interface. *Measurement* 122, 339–346. <https://doi.org/10.1016/j.measurement.2018.03.003>
- [33]. Tao, G., Yuan, J., Chen, Q., Peng, W., Yu, R., Basack, S., 2021. Chemical stabilization of calcareous sand by polyurethane foam adhesive. *Construction and Building Materials* 295, 123609. <https://doi.org/10.1016/j.conbuildmat.2021.123609>
- [34]. Tavakol, K., Bayat, M., Nadi, B., Ajalloeian, R., 2023. Combined Influences of Cement, Rice Husk Ash and Fibre on the Mechanical Characteristics of a Calcareous Sand. *KSCE J Civ Eng.* <https://doi.org/10.1007/s12205-023-0695-7>

- [35]. Uesugi, M., Kishida, H., 1986. Frictional Resistance at Yield between Dry Sand and Mild Steel. *Soils and Foundations* 26, 139–149. [https://doi.org/10.3208/sandf1972.26.4\\_139](https://doi.org/10.3208/sandf1972.26.4_139)
- [36]. Vangla, P., Latha Gali, M., 2016. Effect of particle size of sand and surface asperities of reinforcement on their interface shear behaviour. *Geotextiles and Geomembranes* 44, 254–268. <https://doi.org/10.1016/j.geotexmem.2015.11.002>
- [37]. Vieira, C.S., Lopes, C.S., Caldeira, L., 2013. Soil-Geosynthetic Interface Shear Strength by Simple and Direct Shear Tests Détermination de la résistance au cisaillement de l' interface sol – géosynthétique par des essais de cisaillement simple et direct, in: *In Proceedings of the 18th International Conference on Soil Mechanics and Geotechnical Engineering*. pp. 3497–3500.
- [38]. Wang, R., Guo, J., Lei, S., Wang, X., Rong, W., Yu, Z., 2022. A study on the cyclic shear and particle breakage characteristics of the interface between steel and calcareous sand. *Marine Georesources and Geotechnology*. <https://doi.org/10.1080/1064119X.2022.2146024>
- [39]. Wang, X.Z., Wang, X.Z., Zhu, C.Q., Meng, Q.S., 2019. Shear tests of interfaces between calcareous sand and steel. *Marine Georesources and Geotechnology* 37, 1095–1104. <https://doi.org/10.1080/1064119X.2018.1529845>
- [40]. Wang, Z., Richwien, W., 2002. A Study of Soil-Reinforcement Interface Friction. *Journal of Geotechnical and Geoenvironmental Engineering* 128, 92–94. [https://doi.org/10.1061/\(asce\)1090-0241\(2002\)128:1\(92\)](https://doi.org/10.1061/(asce)1090-0241(2002)128:1(92))
- [41]. Xiao, S., Suleiman, M.T., Al-Khawaja, M., 2019. Investigation of effects of temperature cycles on soil-concrete interface behavior using direct shear tests. *Soils and Foundations* 59, 1213–1227. <https://doi.org/10.1016/j.sandf.2019.04.009>
- [42]. Xu, L., Wang, R., Xu, D., Wang, J., Wang, X., Meng, Q., 2022. Interface Shear Behavior of Geogrid-Reinforced Calcareous Sand Under Large-Scale Monotonic Direct Shear. *International Journal of Geosynthetics and Ground Engineering* 8. <https://doi.org/10.1007/s40891-022-00403-0>
- [43]. Yavari, N., Tang, A.M., Pereira, J.M., Hassen, G., 2016. Effect of temperature on the shear strength of soils and the soil–structure interface. *Canadian Geotechnical Journal* 53, 1186–1194. <https://doi.org/10.1139/cgj-2015-0355>